

**This is the preprint of the contribution published as:**

Zherebker, A., Rukhovich, G.D., Sarycheva, A., **Lechtenfeld, O.J.**, Nikolaev, E.N. (2022):  
Aromaticity index with improved estimation of carboxyl group contribution for  
biogeochemical studies  
*Environ. Sci. Technol.* **56** (4), 2729 - 2737

**The publisher's version is available at:**

<http://dx.doi.org/10.1021/acs.est.1c04575>

1 **Aromaticity index with improved estimation of carboxyl group contribution for**  
2 **biogeochemical studies**

3 Alexander Zhrebker,<sup>\*a</sup> Gleb D. Rukhovich<sup>a</sup>, Anastasia Sarycheva<sup>a</sup>, Oliver J. Lechtenfeld<sup>\*b</sup>,  
4 Evgeny N. Nikolaev<sup>a</sup>

5 <sup>a</sup> Skolkovo Institute of Science and Technology, 121205, Moscow, Russia. E-mail:

6 [a.zhrebker@skoltech.ru](mailto:a.zhrebker@skoltech.ru)

7 <sup>b</sup> Department of Analytical Chemistry, Research Group BioGeoOmics, Helmholtz Centre for

8 Environmental Research - UFZ, Leipzig DE-04318, Germany. E-mail: [oliver.lechtenfeld@ufz.de](mailto:oliver.lechtenfeld@ufz.de)

9

10 **Abstract**

11 Natural organic matter (NOM) components measured with ultra-high resolution mass spectrometry  
12 are often assessed by molecular formula-based indices, particularly related to their aromaticity, which  
13 are further used as proxies to explain biogeochemical reactivity. An aromaticity index was proposed  
14 to account for hereto-atom contribution to double bonds, but relies on assumptions particularly with  
15 respect to carboxylic acids, abundant functional groups in NOM components. Here, we propose a new  
16 constrained aromaticity index ( $AI_{con}$ ) based on the measured distribution of carboxylic groups among  
17 individual components of NOM which was obtained by deuteromethylation and Fourier-transform ion  
18 cyclotron resonance mass-spectrometry (FTICR MS). Labelling of carboxyl groups in NOM  
19 compounds from diverse sources (coal, marine, peat, permafrost, blackwater river, and soil) revealed  
20 that the most probable number of carboxylic groups was two, which enabled to set a reference point  
21  $n=2$  for carboxyl-accounted  $AI_{con}$  calculation. The proposed index was evaluated against the measured  
22 number of carboxyl groups showing that it provided the smallest errors for aromaticity calculation for  
23 all NOM samples under study as well as for individual natural compounds obtained from the Coconut

24 database, which were significantly less oxidized as compared to NOM. Unlike proposed  $AI_{con}$ ,  
25 conventional AI and  $AI_{mod}$  resulted in significant underestimation of compound aromaticity for both  
26 NOM and individual compounds from the database. In particular,  $AI_{con}$  performed better than  $AI_{mod}$   
27 for all compound classes in which aromatic moieties are expected: aromatics, condensed aromatics  
28 and unsaturated compounds. Therefore,  $AI_{con}$  referenced with two carboxyl groups is preferred over  
29 conventional AI and  $AI_{mod}$  for biogeochemical studies where the aromaticity of compounds is  
30 important to understand the transformations and fate of NOM compounds.

31 **Keywords** NOM, humic substances, FTICR MS, carboxylic groups, aromaticity index,  
32 deuteromethylation, isotopic labeling

33 **Synopsis** Enumeration of carboxylic groups enabled to refine aromaticity index, which is used in  
34 majority of environmental studies engaging mass spectrometry.

## 35 INTRODUCTION

36 Natural organic matter (NOM) and humic substances (HS) are ubiquitous in various  
37 environments, for example, freshwater and marine systems, permafrost and agricultural soils with  
38 extensive biodegradation processes, as well as in caustobiolithes. This makes them an important part  
39 of the global carbon cycle and many studies are devoted to the mechanisms of NOM formation,  
40 transformation and storage.<sup>1,2</sup> The rates and the extent of transformation of these forms of organic  
41 matter (OM) depend on environmental conditions (e.g. the availability of oxygen) and the source  
42 biomass composition.<sup>3,4</sup> However, diagenesis ultimately leads to the accumulation of aromatic and/or  
43 oxygen-rich structures, which are resistant towards further biodegradation and the extent of  
44 degradation can be evaluated by the aromaticity of NOM samples. This concept was developed from  
45 a vast number of studies utilizing the optical properties of NOM and HS (mainly absorbance and  
46 fluorescence). For example, UV/Vis absorbance is commonly used to characterize both the chemical  
47 characteristics (molecular weight or aromaticity) and the dynamics of OM.<sup>5</sup> Several indices were  
48 proposed to characterize aromaticity and the degree of OM transformation: ratio of absorbance values  
49 at 465 and 665 nm ( $E_4/E_6$  ratio), long-wavelength slope of absorption spectrum, fluorescence index<sup>6</sup>  
50 and fluorescence spectrum asymmetry.<sup>7</sup> However, optical indices only reflect the mean or bulk  
51 character of OM based on empirical relationships. To reveal molecular-level transformation during  
52 biogeochemical processing and diagenesis, methods are required which directly assess the aromatic  
53 and aliphatic building blocks of NOM and HS.

54 In this regard,  $^1\text{H}$ ,  $^{13}\text{C}$  and 2D NMR spectroscopy is highly suited to provide quantitative and  
55 qualitative information about aromatic moieties in molecules. Depending on the experiment, it is  
56 possible to determine the contribution of aromatic carbon atoms, aromatic protons and specific  
57 functional groups and their chemical environment.<sup>8</sup> However, in case of complex mixtures like NOM  
58 and HS this information cannot be broken down to the individual molecular level due to broad peaks

59 from significant overlap of chemical shifts.<sup>9</sup> Recently Bell with co-workers revealed possible aromatic  
60 moieties from lignin in peat humic substances via combining <sup>13</sup>C isotopic labeling and specific  
61 spectrum-acquisition conditions (*pseudo* 4D-NMR).<sup>10</sup>

62 Mass spectrometry (MS), in contrast to NMR, provides information on a single molecular  
63 composition by determination its exact molecular mass of ions and their structural fragments. For  
64 example, reduction of polar components from Suwannee River Fulvic Acid (SRFA, an OM reference  
65 standard) followed by 2D gas-chromatography (GC) coupled to time-of-flight mass spectrometry  
66 enabled to determine isomeric alicyclic hydrocarbons and terpenoids.<sup>11</sup> However, GC-MS analysis is  
67 mostly limited to aliphatic compound and not easily applicable for aromatic and polar species. Hence,  
68 NOM and HS studies mostly utilize direct infusion (DI) of dissolved samples using soft ionization  
69 methods like electrospray ionization (ESI) coupled to ultra-high resolution mass spectrometry  
70 UHRMS (e.g. Fourier-transform ion cyclotron resonance (FTICR) and Orbitrap mass spectrometry),  
71 which routinely resolve thousands of exact molecular compositions in a single sample.<sup>9,12-14</sup> Despite  
72 sufficient mass resolution provided of UHRMS, tandem mass-spectrometry analysis of NOM and HS  
73 mixtures is challenging and not routinely applied for such mixtures<sup>15,16</sup>. At the same time each  
74 molecular composition detected by UHRMS may correspond to a large number of structural isomers<sup>17</sup>  
75 and only limited formula-based structural information may be derived from these experiments.

76 One example is the formula-based estimation of component aromaticity, which is related to  
77 the unsaturation state of molecules. Aromaticity estimation is widely used and often connected with  
78 optical properties<sup>18</sup> (e.g. correlation with optical density attributed to aromatic chromophores),  
79 chemical properties<sup>19</sup> (e.g. photo-lability) and in biological experiments in which microorganisms  
80 transform components of NOM.<sup>20</sup> For highly aromatic samples (e.g. coal, petroleum, etc.),  
81 aromaticity is correlated to double bond equivalent (DBE) and the DBE/C ratio where e.g. condensed  
82 aromatic structures require  $DBE/C \geq 0.7$ .<sup>21</sup> For organic aerosol the aromaticity equivalent ( $X_c$ ) was  
83 proposed to attribute compounds to aromatic and condensed aromatic species by subtracting from

84 DBE the number of mathematically possible CH<sub>2</sub> fragments.<sup>22</sup> For heteroatom-rich NOM, aromaticity  
85 index (AI) and modified aromaticity index (AI<sub>mod</sub>) were introduced as proxies to account for DBE and  
86 hence aromaticity attributed to carbon skeleton.<sup>23,24</sup> AI and AI<sub>mod</sub> assume that all oxygen atoms and  
87 half of oxygen atoms form double bonds with sp<sup>2</sup>-hybridized carbon, respectively. Sulfur and  
88 nitrogen, in contrast, are always considered to form π-bonds with carbon, both in AI and AI<sub>mod</sub>,  
89 introducing additional uncertainty. The advantage of AI indices over Xc is the normalized range from  
90 0 to 1. AI is considered as the most conservative aromatic system approximation for NOM/HS and  
91 despite some uncertainties of these indices, AI and AI<sub>mod</sub> currently serve as major structural  
92 parameters in many geochemical studies of NOM/HS<sup>4,18,25</sup>.

93 In our opinion, due to the fact that estimation of molecule aromaticity is often connected to  
94 presumed biological and chemical properties of NOM in biogeochemical studies, this approach  
95 resulted in appearance of important issues in the field. For example, AI thresholds are used as direct  
96 marker of the presence or absence of aromatic units in molecules and not as measure of “mean”  
97 aromaticity as it has been proposed in the original paper by Koch and Dittmar<sup>23,24</sup>. For example,  
98 phenols with saturated substituents might be excluded from the list of aromatic components assigned  
99 by AI or AI<sub>mod</sub> values while from the chemical point of view they are aromatic and characterized by  
100 all chemical properties of aromatic compounds. In addition, we have shown that molecules with the  
101 same low AI<sub>mod</sub> value (e.g. 0.3) may correspond to isomers with and without aromatic rings depending  
102 on the geochemical origin.<sup>26</sup> Hence, conclusions about aromatic character of molecules and its  
103 connection to reactivity in environment can easily be false. One of the reason for the false-assignment  
104 of structures using AI or AI<sub>mod</sub> is the underestimation of phenolic and methoxy-groups, which are  
105 abundant in terrestrial NOM samples and supposedly rare in marine DOM and microbial-derived  
106 samples.<sup>27</sup> Another problem is that originally NMR-based distribution of carbon-oxygen bonds in  
107 marine DOM was directly used to estimate number of COOH groups for FTICR MS-based AI<sub>mod</sub>.<sup>23</sup>  
108 However, such approximation ignores issues of using NMR versus DI ESI MS, since the latter ionizes

109 only a part of the sample with possible distortion of relative intensities: e.g. charge suppression during  
110 ionization<sup>28</sup> and selectivity of ESI<sup>29,30</sup> have been reported. Hence, a refinement of formula-based  
111 aromaticity index is needed.

112 The objective of this study was to explore the distribution of carboxyl groups among individual  
113 components of NOM and HS of different origin and to provide a better evidence-based aromaticity  
114 index calculated with the information on the COOH groups. Despite other functional groups are  
115 integrally presented in NOM<sup>31</sup>, the detailed labeling experiments confirmed that next to carbon-  
116 backbone (C=C) carboxylic groups (C[=O]OH) contributed most to DBE. Hence, estimation of the  
117 number of carboxylic groups will enable to provide a better approximation for molecule aromaticity.

## 118 **MATERIALS AND METHODS**

119 Solvents and other reagents used in this study were commercially available. Methanol of  
120 HPLC grade (Lab-Scan) was used for elution and dissolution of sample. High-purity distilled water  
121 (18.2 MΩ) was prepared using a Millipore Simplicity 185 system. D-enrichment of deuterated  
122 methanol (CD<sub>3</sub>OD). Bond Elut PPL (Priority PolLutant, Agilent Technologies) cartridges (50 mg, 1  
123 mL) were used for isolation and purification of the parent and the labeled samples. PPL represents a  
124 modified styrene-divinylbenzene polymer designed for polar organic compounds extraction. Raw  
125 mass-spectrometric data for deuteromethylated samples of various origin were obtained from the  
126 previous studies.<sup>26,31,32</sup> Additionally, top soil pore water from a riparian zone in a headwater catchment  
127 (Bavarian Forest National Park, Germany) and North Sea water (54.132670°N, 7.891330°E) were  
128 analyzed using deuteromethylation method. The list of all samples and their description is presented  
129 in Table S1. The number of assigned CHO-only and other formulae are presented in Tables S2.

### 130 **Labeling procedures**

131 Carboxylic groups in the parent samples were selectively deuteromethylated following the previously  
132 developed regioselective method.<sup>32</sup> Briefly: SOCl<sub>2</sub> (60 μL) was added dropwise to a solution of 0.5

133 mg of OM in 1.5 mL CD<sub>3</sub>OD under continued stirring and ice-cooling. The reaction mixture was then  
134 refluxed for 4 h (6 h for the marine sample) and dried under vacuum. Solid residue was purified using  
135 solid-phase extraction (SPE) from aqueous solution using styrene-divinylbenzene sorbents (Agilent,  
136 Bond Elut PPL) according to the procedure described for DOM samples.<sup>33</sup>

### 137 **Determination of labeling series by FTICR mass spectrometry**

138 Detailed information on FTICR MS measurements can be found elsewhere.<sup>26,31,32</sup> For COOH-  
139 groups enumeration a Python-based script has been developed which enabled fully automatic  
140 assignment. Similar to previously developed workflow<sup>34</sup> the algorithm includes a juxtaposition of raw  
141 FTICR mass spectra of labeled and parent samples and formulae lists of parent samples with  
142 subtraction of one proton to reproduce m/z value of negative ions. The algorithm facilitates extraction  
143 and enumeration of peak series with mass differences corresponding to the deuteromethylation (m/z  
144 difference of 17.03448) and filtration of the obtained results based in the following heuristic rules for  
145 the number of carboxylic groups ( $n$ ): number of oxygen atoms (O) in molecular formula must be  $\geq$   
146  $2n$ ; in case of a high deuteromethylation yield and the absence of the parent peak, first peak in the  
147 labeling series must correspond to  $n < 3$ ; labeling series must be continuous without gaps; peaks  
148 corresponding to the labeling series must absent in the parent mass spectra (important for peaks with  
149 low intensities); Mass error (between peaks of a labeling series) must be below 0.0003 m/z, which  
150 was optimized based on the FTICR MS instrument performance. The applied algorithm considers  
151 stepwise small moiety addition (i.e. H vs CD<sub>3</sub>) to the ions, enabling fast and robust detection of  
152 labeling series.

### 153 **Data treatment**

154 Visualization of data has been performed with Python library Matplotlib (<https://matplotlib.org/>).  
155 Statistical analysis has been performed with Python libraries numpy and pandas. Three aromaticity  
156 indices were calculated according to equations 1-3. Experimental aromaticity index - AI<sub>exp</sub> was  
157 calculated according to eq. 3 with experimentally determined  $n$ .

158 
$$AI = \frac{1+C-O-0.5H}{C-O} \quad (1)$$

159 
$$AI_{mod} = \frac{1+C-0.5O-0.5H}{C-0.5O} \quad (2)$$

160 
$$AI_{con} = \frac{1+C-(COOH)_n-0.5H}{C-(COOH)_n} \quad (3)$$

### 161 **Natural compounds database**

162 To assess the AI value for individual compounds, a local copy of Collection of Open Natural Products  
163 (Coconut) database<sup>35</sup> was established. For each compound in the database the natural product likeness  
164 (NPL) score was calculated following Ertl et al.<sup>36</sup> The local minimum (0.3) of the distribution of NPL  
165 vales was used to select compounds for further analysis (Fig. S1). For manipulation with structures  
166 from the database a Python library RDkit (<https://www.rdkit.org/>) was used. For each compound the  
167 number of COOH-groups was extracted using fully automated algorithm<sup>37</sup> and AI, AI<sub>mod</sub> and AI<sub>con</sub>  
168 were calculated according to eq. 1-3. Only CHO compounds were considered for further evaluation  
169 to exclude structures, which can not be ionized by the negative ESI.

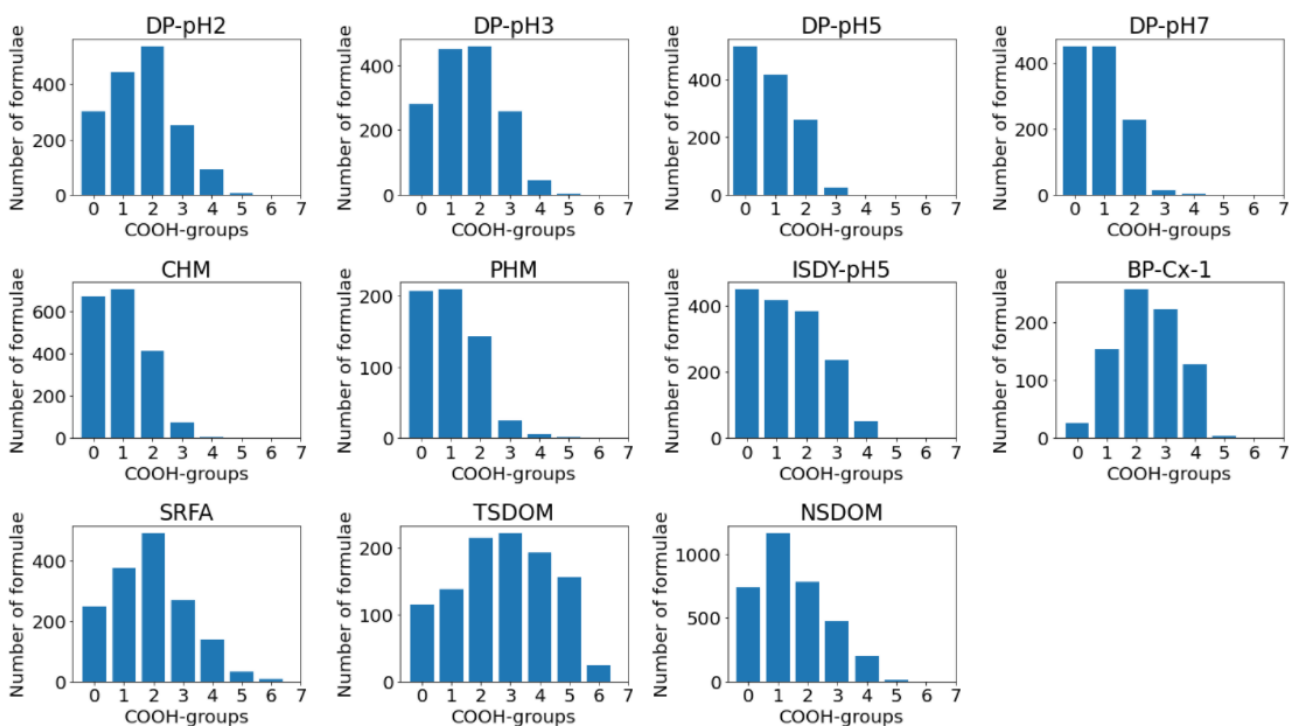
### 170 **In-silico molecular formulae dataset**

171 To further extend the analysis to all possibilities of COOH-functionality regardless of the actual  
172 molecular existence, all possible CHO-molecular compositions were generated in-silico as it has been  
173 described elsewhere.<sup>38</sup> In brief: formulae were generated in the range of molecular weights from 200  
174 to 800 Da using integer atomic weights of elements (e.g. 12, 1, 16). Subsequently, formulae were  
175 filtered according to the typical NOM and HS compositional space -  $0.27 \leq H/C \leq 2.2$ ,  $0 < O/C \leq 1$ <sup>39</sup>  
176 and Senior's rules, which estimate the plausibility of chemical graph existence.<sup>40</sup> This resulted in  
177 21,617 CHO formulae in the test dataset. Additionally, to each individual formula all possible numbers  
178 of carboxylic groups were assigned (Table S3). For example, molecule with five oxygen atoms in  
179 formula may contain zero, one and two COOH-groups in its structure and all three cases were added  
180 to the dataset. AI, AI<sub>mod</sub> and AI<sub>con</sub> were calculated according to eq. 1-3 for the whole dataset.

## 181 RESULTS AND DISCUSSION

### 182 Distribution of carboxylic groups in HS and NOM samples

183 We collected data for eleven samples from different origins (coal, marine, peat, permafrost, black-  
184 water river, and soil) cover a broad range of molecular composition and structural diversity (Table  
185 S1). The distributions of experimentally determined COOH-groups are shown in Fig. 1 for all samples.  
186 In all cases carboxylic groups were assigned to over one thousand molecular formulae based on CD<sub>3</sub>-  
187 labeling and their distribution in the molecular H/C vs O/C space are shown in Fig. S2. For terrestrial  
188 samples isolated from peat and coal the majority of compounds possessed between zero and two  
189 carboxylic groups. A similar result was obtained for soil extracts but its fractions isolated at pH 2 and  
190 pH 3 included also higher number of formulae with three and four carboxylic groups. Surprisingly,  
191 synthetic BP-Cx sample obtained by oxidation of lignin hydrolysate was dominated by species with  
192 two to four COOH-groups, which indicates drastic oxidation of primary alcohols in lignin moieties  
193 during reaction.<sup>41</sup> Top soil porewater (TSDOM) contained the largest number of polycarboxylic acids  
194 while marine (NSDOM) and riverine (SRFA) DOM also contained a wide range of molecules with  
195 up to six COOH-groups. It should be noted that peak series from deuteromethylation typically consist  
196 of multiple ions with different numbers of COOH.<sup>32</sup> The contribution of isomers (with variable  
197 number of COOH groups) to the observed peak series cannot be elaborated without applying  
198 chromatography or other separation methods.<sup>42-44</sup> Therefore, the experimental setup used in this study  
199 results in an upper estimation of carboxylic group functionality for each formula.



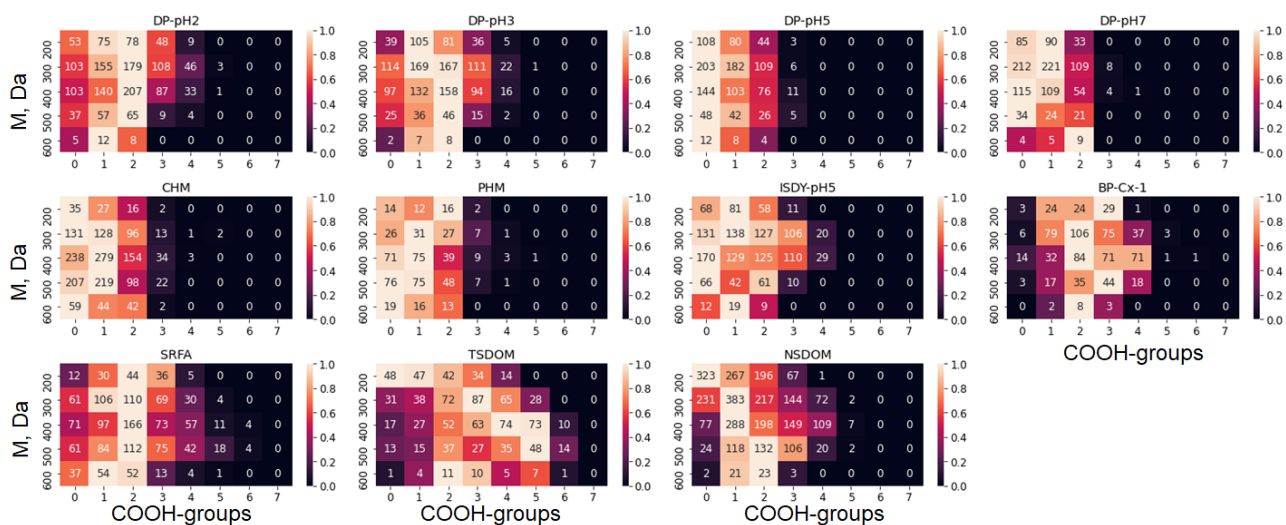
200

201 **Figure 1.** Distribution of carboxylic (COOH) groups in formulae from various NOM and HS samples as  
 202 determined by deuteromethylation and FTICR MS. For a description of the samples refer to Table S1.

203

204 Despite clear differences in carboxylic functionality between samples the maximum of COOH  
 205 distribution correspond to one and two carboxylic groups per molecule for all samples, even for the  
 206 most acidic, which was obtain by acid-base fractionation of soil water extract (DP-pH2; Fig 1).<sup>26</sup>  
 207 Consequently also the overall distribution of COOH in formulae and their contribution to the total  
 208 intensity across all samples revealed overall maxima at one and two COOH-groups (Fig. S3).  
 209 Comparing this to the distribution of oxygen for (all and COOH-assigned) formulae in each sample  
 210 (Fig. S4) and taking into account that most of the NOM components may contains no more than two  
 211 carbonyl groups,<sup>45,46</sup> we conclude an overall high contribution of functional groups with sp<sup>3</sup>-  
 212 hybridized oxygen atoms: alcohols, phenols and ethers explaining the remainder of oxygen atoms  
 213 (Fig. S5). This indicates that in most cases the actual COOH-abundance on OM is highly  
 214 overestimated by AI and AI<sub>mod</sub> (eq. 1-2) and the carbon skeleton aromaticity is likely significantly  
 215 higher than it is deduced even from AI<sub>mod</sub>.<sup>24</sup>

216 In order to deeper examine the estimation of COOH-groups used for conventional AI<sub>mod</sub>,  
 217 formulae distribution with different amount of assigned COOH-groups in formulae was obtained for  
 218 mass ranges between 200 to 800 Da (Fig. 2). The number of COOH-groups is mostly independent on  
 219 the mass and the maximum number of formulae were assigned with two COOH-groups for a broad  
 220 range of masses.



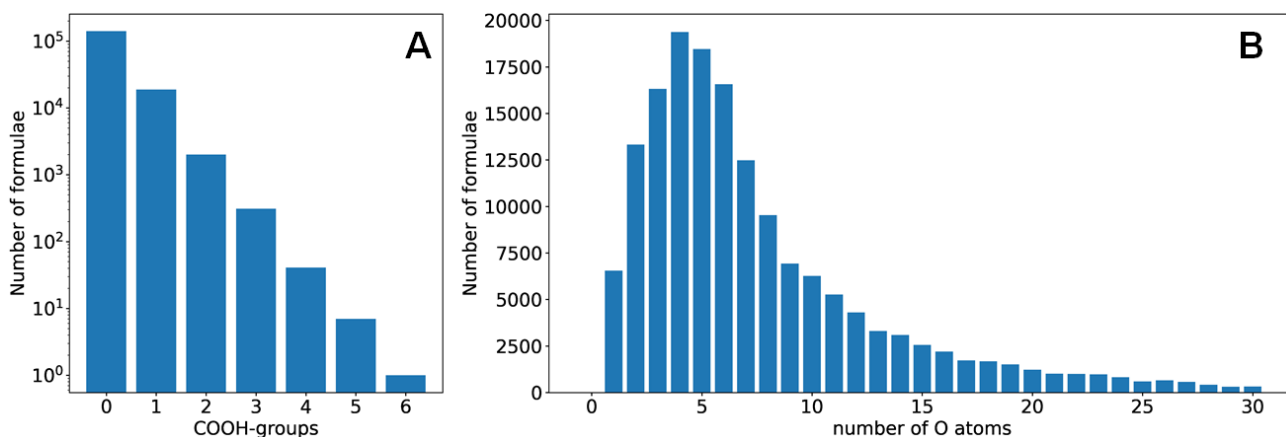
221

222 **Figure 2.** Number of formulae with different number of carboxylic groups as determined by deuteromethylation  
 223 and FTICR MS. Color corresponds to the proportion of the number of COOH-groups (0-7) in each mass range.

224

## 225 Distribution of carboxylic groups in natural compounds

226 In order to further investigate the importance of COOH-functionality determination on aromaticity  
 227 estimation we evaluated compounds in the largest database of individual natural compounds, the  
 228 Coconut database. Only compounds with NPL-score exceeding 0.3 were considered to exclude  
 229 synthetic compounds. The filtered database contained 161 316 structures (only CHO molecules)  
 230 corresponding to 14 485 unique molecular formulae. In fact, most natural compounds in the mass  
 231 range between 100 and 2000 Da do not contain any COOH-group and only a fraction of compounds  
 232 contains one or more COOH (Fig. 3A) although these compounds are overall rich in oxygen (Fig.  
 233 3B).



234

235 **Figure 3.** Distribution of natural compounds from Coconut database<sup>35</sup> according to the number of (A)  
 236 carboxylic groups (note log scale), (B) oxygen atoms.

237

238 Natural products in the Coconut database are by definition non-degraded compounds often  
 239 containing long-aliphatic substituents adjacent to the alicyclic or aromatic cores and non-oxidized  
 240 functional groups – alcohols and even aldehydes. Such saturated compounds are not resistant to  
 241 biodegradation in the environment and may only be found (intact or minor transformed) in permafrost  
 242 NOM, as deduced from NMR spectroscopy studies<sup>47,48</sup> while polyphenols without carboxylic groups  
 243 present in the database are widely distributed in various eco-systems. Overall, NOM and HS were  
 244 characterized by having the highest probability for  $n(\text{COOH}) = 2$ , while COOH-groups are mostly  
 245 absent in individual structures isolated from nature. For further analysis we considered zero and two  
 246 COOH groups as reference points which can be inserted into eq. 3 as number of COOH.

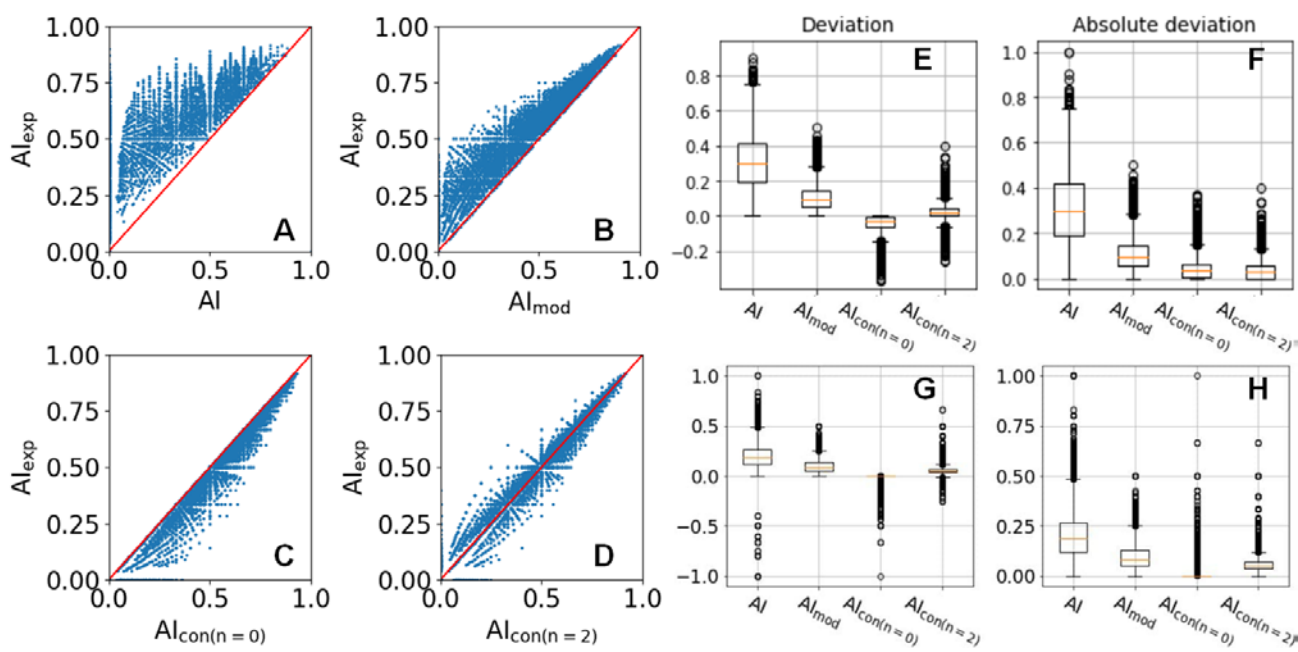
247

### 248 **Carboxylic groups reference points for NOM and HS components aromaticity estimation**

249 For the set of samples for which the number of COOH-groups were experimentally determined, an  
 250 experimental aromaticity index ( $\text{AI}_{\text{exp}}$ ) was derived. This index was further used as reference for  
 251 statistical evaluation of different formula-based, calculated AI indices – AI,  $\text{AI}_{\text{mod}}$  and  $\text{AI}_{\text{con}}$  (eq. 1-3),  
 252 the latter with two values ( $n = 0, 2$ ) for COOH-groups according to the experimentally determined  
 253 COOH-group distributions (Fig. S3). The calculated indices for HS and NOM components are plotted

254 versus experimental aromaticity index  $AI_{exp}$  (Fig. 4A-D). Expectedly, both AI and  $AI_{mod}$  mostly  
255 underestimate the compound aromaticity. Actually, original AI is calculated assuming that all oxygen  
256 atoms are bound to  $sp^2$ -hybridized carbon (i.e. C=O), which strongly reduces the available DBE to  
257 account for aromatic moieties in oxygen-rich NOM formulae. Expectedly for  $AI_{mod}$ , with the  
258 approximation of COOH groups covering all oxygen atoms (eq. 2), aromaticity can be estimated more  
259 accurately than AI, but in most cases experimentally derived aromaticity it is still significantly  
260 underestimated by  $AI_{mod}$ . Interestingly the NSDOM possessed a distinct shift toward lower number  
261 of non-carboxylic oxygen atoms when considering CHO-only formulae (Fig. S5B), corroborating  
262 NMR-based estimates of COOH functionalities for calculate  $AI_{mod}$  for marine DOM. For some  
263 samples there is indeed a connection between COOH-content and oxygen number (e.g. BP-Cx-1 and  
264 TSDOM) and the maximum of the number of formulae for each number of COOH approaches  $O/2$   
265 (Fig. S6), but most of the formulae are still below this upper threshold. The overall best (i.e. most  
266 accurate) approximation of  $AI_{exp}$  was obtained with the constant number of COOH groups ( $n(COOH)$   
267 = 2) in eq. 3, which was chosen as reference point (Fig. 3E,F).

268 Calculation of  $AI_{con}$  using  $n(COOH) = 2$  may result in underestimation of aromaticity, e.g. for  
269 polyphenols with a lack of carboxylic groups. Using  $n(COOH) = 0$  in eq. 3 results in the  
270 transformation of  $AI_{con}$  to trivial DBE/C (in case of CHO), which ignores all oxygenated functional  
271 group with double bonds. Consequently, aromaticity of NOM and HS in that case is strongly  
272 overestimated (Fig. 3C). Despite simplification if using constant value of  $n(COOH)$   $AI_{con}$  provides  
273 significantly better results as compared to  $AI_{mod}$  also for individual, biogeochemically diverse samples  
274 (Fig. S7). Only for the synthetic BP-Cx-1 sample, error distribution of  $AI_{mod}$  was comparable to the  
275  $AI_{con}$  with  $n=2$  whereas even for the marine sample,  $AI_{con}$  with  $n=2$  resulted in a more accurate  
276 estimate as compared to  $AI_{mod}$ .



277

278 **Figure 4.** A-D) Experimental AI index vs estimated aromaticity obtained by eqs. 1-3 with  $n(\text{COOH})$  fixed to 0  
 279 and 2 for eq. 3 for all samples under study. E,F) Error distribution for calculated aromaticity indices for all  
 280 NOM and HS samples combined against experimentally obtained AI. G,H) Error distribution for aromaticity  
 281 indices for all Coconut CHO compounds against structure-derived AI.

282

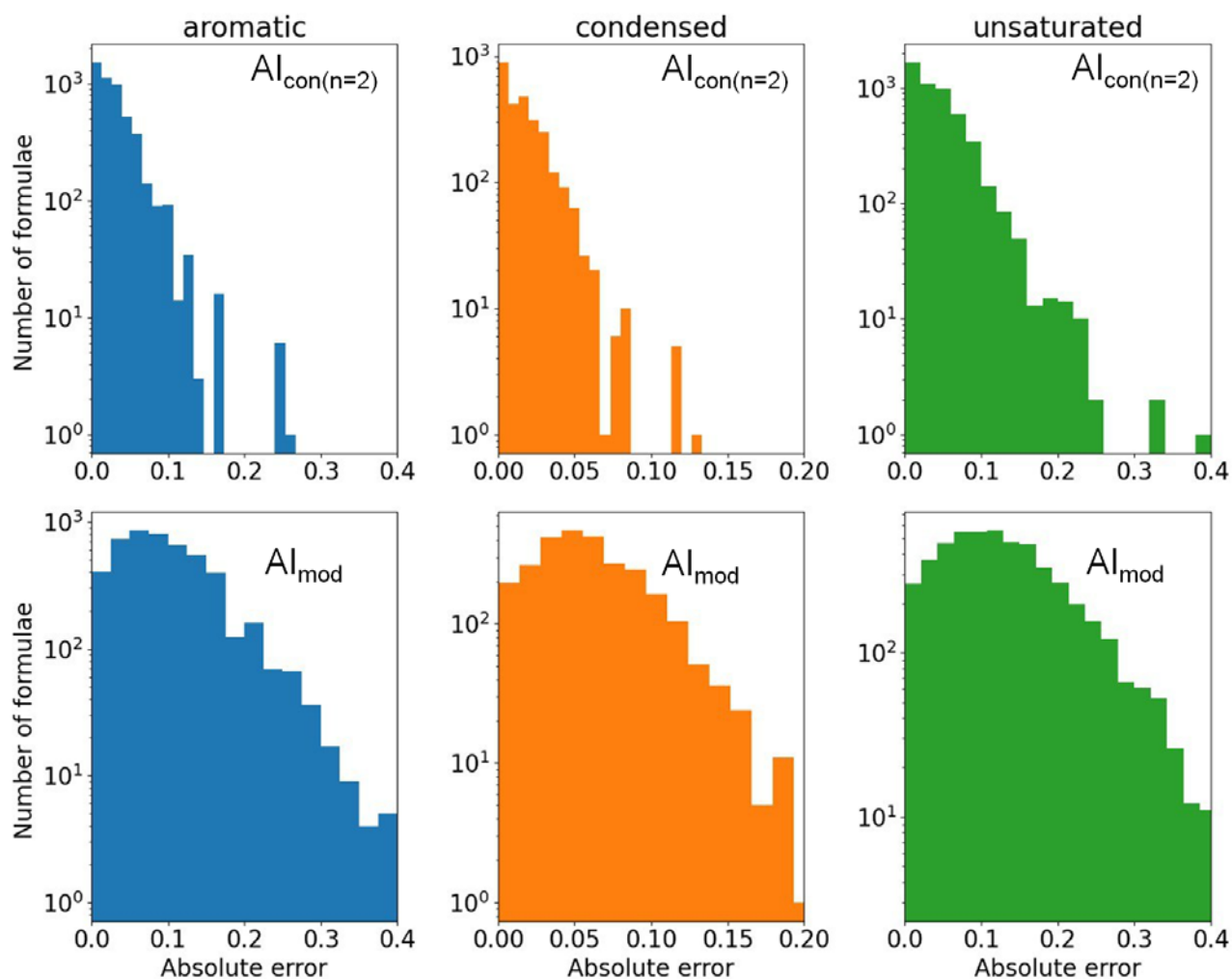
283 The statistical evaluation of aromaticity indices was also performed for the Coconut database,  
 284 in which the number of COOH-groups was directly extracted from the structures. Exact structure-  
 285 derived aromaticity index vs estimated aromaticity plots are presented in Fig. S8 and the  
 286 corresponding error distribution shown in Fig. 4(G,H). Obviously,  $AI_{con}$  with  $n(\text{COOH}) = 0$  yielded  
 287 best results since the prevailing number of structures in Coconut are devoid of carboxylic groups.  
 288 However, taking into account that most of the database compounds are less oxidized as compared to  
 289 NOM and HS it was of interest to examine conventional AI and  $AI_{mod}$  for natural compounds. Clearly,  
 290 approximations of AI and  $AI_{mod}$  result in significant error in aromaticity estimations. The absolute  
 291 error exceed 0.3 for  $AI_{mod}$  in many cases but the third quartile of the error distribution is less for the  
 292 Coconut database compounds than for the NOM components. This is explained by the maximum of  
 293 the oxygen distribution (4-5) for Coconut compounds, which corresponds to a small O/2 coefficient  
 294 in eq. 2 for  $AI_{mod}$ .

295 In order to examine the applicability of the proposed carboxyl reference point ( $n(\text{COOH}) = 2$ )  
296 for the entire domain of possible CHO formulae and partially account for formulae present in NOM  
297 which were absent in the current study, the in-silico formulae dataset with all possible values of  
298 COOH-groups was used. Resulting COOH-distribution and statistical assessment are presented in Fig.  
299 S9. As expected, both AI and  $\text{AI}_{\text{mod}}$  underestimated C-C accounted unsaturation of this artificial  
300 dataset, while  $\text{AI}_{\text{con}}$  with  $n(\text{COOH}) = 2$  in eq. 3 resulted in adequate skewness and low median value  
301 of errors. Overall, the results for NOM samples, Coconut database and in-silico dataset for all possible  
302 variants of carboxylic functionality for CHO species strongly suggest that aromaticity can be reliably  
303 estimated for a wide range of natural species from both fresh and degraded organic matter. Overall,  
304 using  $\text{AI}_{\text{con}}$  with  $n=2$  (eq. 3) results significantly smaller errors in sample comparison or even  
305 aromaticity estimate for a single molecular component than conventional  $\text{AI}_{\text{mod}}$ .

### 306 **Estimation of aromaticity for different AI-based classes of NOM and HS**

307 In biogeochemical studies of NOM and HS the suite of molecular formulae of samples is often divided  
308 into different compound classes based on atomic ratios (H/C, O/C) and aromaticity index.<sup>49</sup> This  
309 approach is widely applied, for example, to find correlations between molecular composition and  
310 optical properties of NOM.<sup>19,50,51</sup> Since these compound classes often imply a specific biogeochemical  
311 reactivity, the resulting error of aromaticity estimation of proposed  $\text{AI}_{\text{con}}$  with fixed  $n(\text{COOH}) = 2$  and  
312  $\text{AI}_{\text{mod}}$  with O/2 coefficient for different molecular classes was assessed (Fig. 5). Analysis of three  
313 most abundant compound classes, which may contain aromatic moieties (“aromatics”, “condensed  
314 (aromatics)” and “unsaturated”)<sup>49</sup> highlighted the advantages of the proposed metric ( $\text{AI}_{\text{con}}$  with  
315  $n(\text{COOH}) = 2$ ) over  $\text{AI}_{\text{mod}}$ . Using  $\text{AI}_{\text{con}}$  resulted in a more adequate attribution of formulae to  
316 compound classes even in case of unsaturated compounds, which are often referred as carboxyl-rich  
317 alicyclic molecules (CRAM).<sup>52</sup> For example, Coconut database includes a number of compounds with  
318 terpenoid scaffolds, which are unsaturated but do not contain aromatic rings. At the same time  
319 aromatic compounds with long-chain aliphatic substituents are also abundant. Without structural

320 elucidation it is impossible to distinguish between them, however, experimentally (by enumeration of  
 321 COOH groups) or by calculation of the proposed  $AI_{con}$  with set  $n = 2$  for COOH groups, it is possible  
 322 at least to suggest aromatic moieties while  $AI_{mod}$  does not reliably indicate aromatic structures in such  
 323 cases. Recently, we demonstrated that DOM from permafrost soil contain CRAM type molecules  
 324 while the same molecular formulae in soil DOM from a temperate region was assigned to as aromatic  
 325 compounds.<sup>26</sup>



326

327 **Figure 5.** Absolute error distribution of aromaticity estimation against  $AI_{exp}$  for three classes<sup>49</sup> of NOM and  
 328 HS components, which may contain aromatic moieties, based on atomic ratios and (upper-row panels)  $AI_{con}$   
 329 with set COOH-group number  $n(COOH) = 2$  or  $AI_{mod}$  (lower-row panels).

330

331 In order to evaluate the applicability of the proposed  $AI_{con}$  with  $n=2$ , several points should be  
 332 taken into account. Firstly, in the present work only negative ESI has been considered and applicability

333 of  $AI_{con}$  should be carefully used and tested in case of other ionization techniques. Secondly, setting  
334 of a fixed number for COOH-groups may still result in false conclusions when discussing the structure  
335 of compounds detected by FTICR MS. Here deuteromethylation labeling, MS/MS experiments or  
336 other techniques can be used to more precisely enumerate COOH groups. Additionally, the  
337 conservative attribution of all N,S-atoms to moieties with  $\pi$ -bonds remains disadvantageous and  
338 requires chemical justification. Finally, for different types of samples, the maximum of COOH-  
339 distribution can vary. Therefore, it can be expected that  $AI_{con}$  with variable  $n(COOH)$ -values may  
340 better describe specific types of samples. For example, considering a range of  $n(COOH)$ -values for  
341 CHM and SRFA samples revealed that  $n=1$  is more suitable for the coal sample, and  $n=2$  for the  
342 blackwater river (Fig. S10). However, in the range between 0 and 3,  $AI_{con}$  always resulted in a smaller  
343 error as compared to  $AI_{mod}$  considering experimental derived number of COOH. In conclusion,  $AI_{con}$   
344 with  $n(COOH)=2$  is a robust and precise metric for the mean aromaticity estimation, especially for  
345 CHO-only compounds.  $AI_{con}$ , which can be easily calculated from molecular formulae, can substitute  
346 conventional AI and  $AI_{mod}$  as a working metric for biogeochemical researches including NOM and  
347 HS with different degree of microbial and oxidative transformations.

## 348 **ASSOCIATED CONTENT**

### 349 **Supporting Information**

350 Additional experimental data, sample description, COOH and oxygen atoms distributions, including  
351 examination of aromaticity index for each sample, and Table S3 with in-silico generated CHO  
352 molecular compositions with theoretically assigned COOH-group numbers.

### 353 **Acknowledgments**

354 This work was supported by Russian Science Foundation grant 21-47-04405 and the German  
355 Research Foundation (grant 445025664). The authors are grateful to Maria P. da Silva (UFZ) for  
356 providing the soil pore-water, Boris P. Koch (AWI) for providing and Rebecca Matos (UFZ) for

357 labelling the marine sample, and for using the analytical facilities of the Centre for Chemical  
358 Microscopy (ProVIS) at the Helmholtz Centre for Environmental Research, Leipzig which is  
359 supported by the European Regional Development Funds (EFRE - Europe funds Saxony) and the  
360 Helmholtz Association. AZ, GDR and EN acknowledge support from the European's Horizon 2020  
361 Research and Innovation Program under grant agreement No. 731077

### 362 **Competing financial interest**

363 The authors declare no competing financial interests.

### 364 **References**

- 365 (1) D'Andrilli, J.; Cooper, W. T.; Foreman, C. M.; Marshall, A. G. An Ultrahigh-Resolution  
366 Mass Spectrometry Index to Estimate Natural Organic Matter Lability. *Rapid Commun. Mass*  
367 *Spectrom.* **2015**, *29* (24), 2385–2401.
- 368 (2) Yuan, C.; Sleighter, R. L.; Weavers, L. K.; Hatcher, P. G.; Chin, Y. P. Fast  
369 Photomineralization of Dissolved Organic Matter in Acid Mine Drainage Impacted Waters.  
370 *Environ. Sci. Technol.* **2019**, *53* (11), 6273–6281.
- 371 (3) Waggoner, D. C.; Wozniak, A. S.; Cory, R. M.; Hatcher, P. G. The Role of Reactive Oxygen  
372 Species in the Degradation of Lignin Derived Dissolved Organic Matter. *Geochim.*  
373 *Cosmochim. Acta* **2017**, *208*, 171–184.
- 374 (4) Stubbins, A.; Mann, P. J.; Powers, L.; Bittar, T. B.; Dittmar, T.; McIntyre, C. P.; Eglinton, T.  
375 I.; Zimov, N.; Spencer, R. G. M. Low Photolability of Yedoma Permafrost Dissolved Organic  
376 Carbon. *J. Geophys. Res. Biogeosciences* **2017**, *122* (1), 200–211.
- 377 (5) Weishaar, J. L.; Aiken, G. R.; Bergamaschi, B. A.; Fram, M. S.; Fujii, R.; Mopper, K.  
378 Evaluation of Specific Ultraviolet Absorbance as an Indicator of the Chemical Composition  
379 and Reactivity of Dissolved Organic Carbon. *Environ. Sci. Technol.* **2003**, *37* (20), 4702–  
380 4708.

- 381 (6) Ohno, T. Fluorescence Inner-Filtering Correction for Determining the Humification Index of  
382 Dissolved Organic Matter. *Environ. Sci. Technol.* **2002**, *36* (4), 742–746.
- 383 (7) Zsolnay, A.; Baigar, E.; Jimenez, M.; Steinweg, B.; Saccomandi, F. Differentiating with  
384 Fluorescence Spectroscopy the Sources of Dissolved Organic Matter in Soils Subjected to  
385 Drying. *Chemosphere* **1999**, *38* (1), 45–50.
- 386 (8) Zhrebker, A.; Shirshin, E.; Kharybin, O.; Kostyukevich, Y.; Kononikhin, A.; Konstantinov,  
387 A. I.; Volkov, D.; Roznyatovsky, V. A.; Grishin, Y. K.; Perminova, I. V.; Nikolaev, E.  
388 Separation of Benzoic and Unconjugated Acidic Components of Leonardite Humic Material  
389 Using Sequential Solid-Phase Extraction at Different PH Values as Revealed by Fourier  
390 Transform Ion Cyclotron Resonance Mass Spectrometry and Correlation Nuclear Magnetic  
391 Resonance Spectroscopy. *J. Agric. Food Chem.* **2018**, *66* (46), 12179–12187.
- 392 (9) Hertkorn, N.; Ruecker, C.; Meringer, M.; Gugisch, R.; Frommberger, M.; Perdue, E. M.;  
393 Witt, M.; Schmitt-Kopplin, P. High-Precision Frequency Measurements: Indispensable Tools  
394 at the Core of the Molecular-Level Analysis of Complex Systems. *Anal. Bioanal. Chem.*  
395 **2007**, *389* (5), 1311–1327.
- 396 (10) Bell, N. G. A.; Michalchuk, A. A. L.; Blackburn, J. W. T.; Graham, M. C.; Uhrin, D. Isotope-  
397 Filtered 4D NMR Spectroscopy for Structure Determination of Humic Substances. *Angew.*  
398 *Chem. Int. Ed. Engl.* **2015**, *54* (29), 8382–8385.
- 399 (11) Arakawa, N.; Aluwihare, L. Direct Identification of Diverse Alicyclic Terpenoids in  
400 Suwannee River Fulvic Acid. *Environ. Sci. Technol.* **2015**, *49* (7), 4097–4105.
- 401 (12) Spranger, T.; Pinxteren, D. Van; Reemtsma, T.; Lechtenfeld, O. J.; Herrmann, H. 2D Liquid  
402 Chromatographic Fractionation with Ultra-High Resolution MS Analysis Resolves a Vast  
403 Molecular Diversity of Tropospheric Particle Organics. *Environ. Sci. Technol.* **2019**, *53* (19),  
404 11353–11363.
- 405 (13) Hawkes, J. A.; Dittmar, T.; Patriarca, C.; Tranvik, L.; Bergquist, J. Evaluation of the Orbitrap

- 406 Mass Spectrometer for the Molecular Fingerprinting Analysis of Natural Dissolved Organic  
407 Matter. *Anal. Chem.* **2016**, *88* (15), 7698–7704.
- 408 (14) Smith, D. F.; Podgorski, D. C.; Rodgers, R. P.; Blakney, G. T.; Hendrickson, C. L. 21 Tesla  
409 FT-ICR Mass Spectrometer for Ultrahigh-Resolution Analysis of Complex Organic Mixtures.  
410 *Anal. Chem.* **2018**, *90* (3), 2041–2047.
- 411 (15) Witt, M.; Fuchser, J.; Koch, B. P. Fragmentation Studies of Fulvic Acids Using Collision  
412 Induced Dissociation Fourier Transform Ion Cyclotron Resonance Mass Spectrometry. *Anal.*  
413 *Chem.* **2009**, *81* (7), 2688–2694.
- 414 (16) Nebbioso, A.; Piccolo, A. Basis of a Humeomics Science: Chemical Fractionation and  
415 Molecular Characterization of Humic Biosuprastructures. *Biomacromolecules* **2011**, *12* (4),  
416 1187–1199.
- 417 (17) Hertkorn, N.; Frommberger, M.; Witt, M.; Koch, B. P.; Schmitt-Kopplin, P.; Perdue, E. M.  
418 Natural Organic Matter and the Event Horizon of Mass Spectrometry. *Anal. Chem.* **2008**, *80*  
419 (23), 8908–8919.
- 420 (18) Gonsior, M.; Peake, B. M.; Cooper, W. T.; Podgorski, D.; D’Andrilli, J.; Cooper, W. J.  
421 Photochemically Induced Changes in Dissolved Organic Matter Identified by Ultrahigh  
422 Resolution Fourier Transform Ion Cyclotron Resonance Mass Spectrometry. *Environ. Sci.*  
423 *Technol.* **2009**, *43* (3), 698–703.
- 424 (19) Stubbins, A.; Spencer, R. G. M.; Chen, H.; Hatcher, P. G.; Mopper, K.; Hernes, P. J.;  
425 Mwamba, V. L.; Mangangu, A. M.; Wabakanghanzi, J. N.; Six, J. Illuminated Darkness:  
426 Molecular Signatures of Congo River Dissolved Organic Matter and Its Photochemical  
427 Alteration as Revealed by Ultrahigh Precision Mass Spectrometry. *Limnol. Oceanogr.* **2010**,  
428 *55* (4), 1467–1477.
- 429 (20) Spencer, R. G. M.; Mann, P. J.; Dittmar, T.; Eglinton, T. I.; McIntyre, C.; Holmes, R. M.;  
430 Zimov, N.; Stubbins, A. Detecting the Signature of Permafrost Thaw in Arctic Rivers.

- 431 *Geophys. Res. Lett.* **2015**, 42 (8), 2830–2835.
- 432 (21) Hockaday, W. C.; Grannas, A. M.; Kim, S.; Hatcher, P. G. Direct Molecular Evidence for the  
433 Degradation and Mobility of Black Carbon in Soils from Ultrahigh-Resolution Mass Spectral  
434 Analysis of Dissolved Organic Matter from a Fire-Impacted Forest Soil. *Org. Geochem.*  
435 **2006**, 37 (4), 501–510.
- 436 (22) Yassine, M. M.; Harir, M.; Dabek-Zlotorzynska, E.; Schmitt-Kopplin, P. Structural  
437 Characterization of Organic Aerosol Using Fourier Transform Ion Cyclotron Resonance Mass  
438 Spectrometry: Aromaticity Equivalent Approach. *Rapid Commun. Mass Spectrom.* **2014**, 28  
439 (22), 2445–2454.
- 440 (23) Koch, B. P.; Dittmar, T. From Mass to Structure: An Aromaticity Index for High-Resolution  
441 Mass Data of Natural Organic Matter. *Rapid Commun. Mass Spectrom.* **2006**, 20 (5), 926–  
442 932.
- 443 (24) Koch, B. P.; Dittmar, T. Erratum: From Mass to Structure: An Aromaticity Index for High-  
444 Resolution Mass Data of Natural Organic Matter (Rapid Communications in Mass  
445 Spectrometry (2006) 20 (926-932) DOI: 10.1002/Rcm.2386). *Rapid Communications in Mass  
446 Spectrometry.* 2016, p 250.
- 447 (25) Zhrebker, A.; Podgorski, D. C.; Kholodov, V. A.; Orlov, A. A.; Yaroslavtseva, N. V.;  
448 Kharybin, O.; Kholodov, A.; Spector, V.; Spencer, R. G. M.; Nikolaev, E.; Perminova, I.V.  
449 The Molecular Composition of Humic Substances Isolated From Yedoma Permafrost and  
450 Alas Cores in the Eastern Siberian Arctic as Measured by Ultrahigh Resolution Mass  
451 Spectrometry. *J. Geophys. Res. Biogeosciences* **2019**, 124 (8), 2432–2445.
- 452 (26) Zhrebker, A.; Shirshin, E.; Rubekina, A.; Kharybin, O.; Kononikhin, A.; Kulikova, N. A.;  
453 Zaitsev, K. V.; Roznyatovsky, V. A.; Grishin, Y. K.; Perminova, I. V.; Nikolaev, E. Optical  
454 Properties of Soil Dissolved Organic Matter Are Related to Acidic Functions of Its  
455 Components as Revealed by Fractionation, Selective Deuteromethylation, and Ultrahigh

- 456 Resolution Mass Spectrometry. *Environ. Sci. Technol.* **2020**, *54* (5), 2667–2677.
- 457 (27) Aeschbacher, M.; Graf, C.; Schwarzenbach, R. P.; Sander, M. Antioxidant Properties of  
458 Humic Substances. *Environ. Sci. Technol.* **2012**, *46* (9), 4916–4925.
- 459 (28) Rodgers, R. P.; Mapolelo, M. M.; Robbins, W. K.; Chacón-Patiño, M. L.; Putman, J. C.;  
460 Niles, S. F.; Rowland, S. M.; Marshall, A. G. Combating Selective Ionization in the High  
461 Resolution Mass Spectral Characterization of Complex Mixtures. *Faraday Discuss.* **2019**,  
462 *218*, 29–51.
- 463 (29) Hockaday, W. C.; Purcell, J. M.; Marshall, A. G.; Baldock, J. A.; Hatcher, P. G. Electrospray  
464 and Photoionization Mass Spectrometry for the Characterization of Organic Matter in Natural  
465 Waters: A Qualitative Assessment. *Limnol. Oceanogr.* **2009**, *7*, 81–95.
- 466 (30) Nebbioso, A.; Piccolo, A.; Spiteller, M. Limitations of Electrospray Ionization in the Analysis  
467 of a Heterogeneous Mixture of Naturally Occurring Hydrophilic and Hydrophobic  
468 Compounds. *Rapid Commun. Mass Spectrom.* **2010**, *24* (21), 3163–3170.
- 469 (31) Zhrebker, A.; Lechtenfeld, O. J.; Sarycheva, A.; Kostyukevich, Y.; Kharybin, O.; Fedoros,  
470 E. I.; Nikolaev, E. N. Refinement of Compound Aromaticity in Complex Organic Mixtures  
471 by Stable Isotope Label Assisted Ultrahigh-Resolution Mass Spectrometry. *Anal. Chem.*  
472 **2020**, *92* (13), 9032–9038.
- 473 (32) Zhrebker, A.; Kostyukevich, Y.; Kononikhin, A.; Kharybin, O.; Konstantinov, A. I.; Zaitsev,  
474 K. V.; Nikolaev, E.; Perminova, I. V. Enumeration of Carboxyl Groups Carried on Individual  
475 Components of Humic Systems Using Deuteromethylation and Fourier Transform Mass  
476 Spectrometry. *Anal. Bioanal. Chem.* **2017**, *409* (9), 2477–2488.
- 477 (33) Dittmar, T.; Koch, B.; Hertkorn, N.; Kattner, G. A Simple and Efficient Method for the Solid-  
478 Phase Extraction of Dissolved Organic Matter (SPE-DOM) from Seawater. *Limnol. Ocean.*  
479 *Methods* **2008**, *6*, 230–235.
- 480 (34) Kostyukevich, Y.; Kononikhin, A.; Zhrebker, A.; Popov, I.; Perminova, I.; Nikolaev, E.

- 481 Enumeration of Non-Labile Oxygen Atoms in Dissolved Organic Matter by Use of  $^{16}\text{O}/^{18}\text{O}$   
482 Exchange and Fourier Transform Ion-Cyclotron Resonance Mass Spectrometry. *Anal.*  
483 *Bioanal. Chem.* **2014**, *406* (26), 6655–6664.
- 484 (35) Sorokina, M.; Merseburger, P.; Rajan, K.; Yirik, M. A.; Steinbeck, C. COCONUT Online:  
485 Collection of Open Natural Products Database. *J. Cheminform.* **2021**, *13* (1).
- 486 (36) Ertl, P.; Roggo, S.; Schuffenhauer, A. Natural Product-Likeness Score and Its Application for  
487 Prioritization of Compound Libraries. *J. Chem. Inf. Model.* **2008**, *48* (1), 68–74.
- 488 (37) Ertl, P. An Algorithm to Identify Functional Groups in Organic Molecules. *J. Cheminform.*  
489 **2017**, *9* (1).
- 490 (38) Orlov, A. A.; Zhrebker, A.; Eletskeya, A. A.; Chernikov, V. S.; Kozlovskaya, L. I.; Zhernov,  
491 Y. V.; Kostyukevich, Y.; Palyulin, V. A.; Nikolaev, E. N.; Osolodkin, D. I.; Perminova, I. V.  
492 Examination of Molecular Space and Feasible Structures of Bioactive Components of Humic  
493 Substances by FTICR MS Data Mining in ChEMBL Database. *Sci. Rep.* **2019**, *9* (1), 1–12.
- 494 (39) Sleighter, R. L.; Hatcher, P. G. *Fourier Transform Mass Spectrometry for the Molecular*  
495 *Level Characterization of Natural Organic Matter: Instrument Capabilities, Applications,*  
496 *and Limitations*; INTECH Open Access Publisher, 2011.
- 497 (40) Kind, T.; Fiehn, O. Seven Golden Rules for Heuristic Filtering of Molecular Formulas  
498 Obtained by Accurate Mass Spectrometry. *BMC Bioinformatics* **2007**, *8*.
- 499 (41) Zhrebker, A.; Yakimov, B.; Rubekina, A.; Kharybin, O.; Fedoros, E. I.; Perminova, I. V.;  
500 Shirshin, E.; Nikolaev, E. N. Photoreactivity of Humic-like Polyphenol Material under  
501 Irradiation with Different Wavelengths Explored by FTICR MS and Deuteromethylation.  
502 *Eur. J. Mass Spectrom.* **2020**, *26* (4), 292–300.
- 503 (42) Hawkes, J. A.; Patriarca, C.; Sjöberg, P. J. R.; Tranvik, L. J.; Bergquist, J. Extreme Isomeric  
504 Complexity of Dissolved Organic Matter Found across Aquatic Environments. *Limnol.*  
505 *Oceanogr. Lett.* **2018**, *3* (2), 21–30.

- 506 (43) Leyva, D.; Tose, L. V.; Porter, J.; Wolff, J.; Jaffé, R.; Fernandez-Lima, F. Understanding the  
507 Structural Complexity of Dissolved Organic Matter: Isomeric Diversity. *Faraday Discuss.*  
508 **2019**, *218*, 431–440.
- 509 (44) Stenson, A. C.; Ruddy, B. M.; Bythell, B. J. Ion Molecule Reaction H/D Exchange as a Probe  
510 for Isomeric Fractionation in Chromatographically Separated Natural Organic Matter. *Int. J.*  
511 *Mass Spectrom.* **2014**, *360* (1), 45–53.
- 512 (45) Bianca, M. R.; Baluha, D. R.; Gonsior, M.; Schmitt-Kopplin, P.; Del Vecchio, R.; Blough, N.  
513 V. Contribution of Ketone/Aldehyde-Containing Compounds to the Composition and Optical  
514 Properties of Suwannee River Fulvic Acid Revealed by Ultrahigh Resolution Mass  
515 Spectrometry and Deuterium Labeling. *Anal. Bioanal. Chem.* **2020**, 1–11.
- 516 (46) Baluha, D. R.; Blough, N. V.; Del Vecchio, R. Selective Mass Labeling for Linking the  
517 Optical Properties of Chromophoric Dissolved Organic Matter to Structure and Composition  
518 via Ultrahigh Resolution Electrospray Ionization Mass Spectrometry. *Environ. Sci. Technol.*  
519 **2013**, *47* (17), 9891–9897.
- 520 (47) Pautler, B. G.; Simpson, A. J.; McNally, D. J.; Lamoureux, S. F.; Simpson, M. J. Arctic  
521 Permafrost Active Layer Detachments Stimulate Microbial Activity and Degradation of Soil  
522 Organic Matter. *Environ. Sci. Technol.* **2010**, *44* (11), 4076–4082.
- 523 (48) Perminova, I. V.; Shirshin, E. A.; Konstantinov, A. I.; Zhrebker, A.; Lebedev, V. A.;  
524 Dubinenkov, I. V.; Kulikova, N. A.; Nikolaev, E. N.; Bulygina, E.; Holmes, R. M. The  
525 Structural Arrangement and Relative Abundance of Aliphatic Units May Effect Long-Wave  
526 Absorbance of Natural Organic Matter as Revealed by <sup>1</sup>H NMR Spectroscopy. *Environ. Sci.*  
527 *Technol.* **2018**, *52* (21), 12526–12537.
- 528 (49) Kellerman, A. M.; Dittmar, T.; Kothawala, D. N.; Tranvik, L. J. Chemodiversity of Dissolved  
529 Organic Matter in Lakes Driven by Climate and Hydrology. *Nat. Commun.* **2014**, *5*, 3804.
- 530 (50) Mann, P. J.; Davydova, A.; Zimov, N.; Spencer, R. G. M.; Davydov, S.; Bulygina, E.; Zimov,

- 531 S.; Holmes, R. M. Controls on the Composition and Lability of Dissolved Organic Matter in  
532 Siberia's Kolyma River Basin. *J. Geophys. Res. Biogeosciences* **2012**, *117* (1).
- 533 (51) Kellerman, A. M.; Guillemette, F.; Podgorski, D. C.; Aiken, G. R.; Butler, K. D.; Spencer, R.  
534 G. M. Unifying Concepts Linking Dissolved Organic Matter Composition to Persistence in  
535 Aquatic Ecosystems. *Environ. Sci. Technol.* **2018**, *52* (5), 2538–2548.
- 536 (52) DiDonato, N.; Chen, H.; Waggoner, D.; Hatcher, P. G. Potential Origin and Formation for  
537 Molecular Components of Humic Acids in Soils. *Geochim. Cosmochim. Acta* **2016**, *178*,  
538 210–222.
- 539